Range Dependence of the Optical Communications Channel

Bruce Moision* and William Farr†

ABSTRACT. — We show the capacity of a pulse-position-modulated (PPM) direct-detected optical communications link goes as $1/R^2$ at high signal-to-noise ratio (SNR) and $1/R^4$ at low SNR, where R is the range, and illustrate some consequences of this change in slope. First, we show the capacity is unaffected when the receive diameter is increased and the effective isotropic radiated power (EIRP) decreased in equal proportions, only up to a critical diameter, and that when the receive diameter is larger than this threshold, the receive diameter–EIRP trade-off is unequal (2:1, in dB). Second, we show that this transition in slope implies a crossover in optical and RF capacities as a function of the range, demonstrating the transition for sample deep-space communications links.

I. Introduction

In this article, we examine the range dependence of the capacity of an optical communications channel utilizing pulse-position modulation (PPM) and a direct-detection photon-counting receiver. We show that at high signal-to-noise ratio (SNR), the channel capacity goes as $1/R^2$, where R is the range, and at low SNR the capacity goes as $1/R^4$. The transition between the slopes occurs at the point where background noise power dominates the signal power. A similar behavior was observed in [1], with a transition from the thermal-noise-dominated regime to the signal-noise-dominated regime. We examine a few consequences of this change in slope. First, we show that the capacity is unaffected when the receive diameter is increased and the effective isotropic radiated power (EIRP) decreased in equal proportions, only up to a critical diameter, and that when the receive diameter is larger than this threshold, the receive diameter–EIRP trade-off is unequal (2:1, in dB). Second, we illustrate a crossover of RF and optical capacities as a function of the range (for fixed transmit and receive apertures). This follows under the assumption that an optical system has a larger capacity than its RF counterpart at short ranges (which is typically the case due to the large EIRP gain), the RF system has a $1/R^2$ loss for any R, and the PPM optical capacity transitions at some point to a $1/R^4$ regime. We provide explicit expressions for the range intercepts as a function of the system parameters. A comparison of current state-of-the-art terminals is made, illustrating where current RF and optical systems gain over their counterparts. In a related study in [2], the authors compare RF and optical capacities under a

* Google, Inc.; formerly Communications Architectures and Research Section.
† Flight Communications Systems Section.

The research described in this publication was carried out by the Jet Propulsion Laboratory, California Institute of Technology, under a contract with the National Aeronautics and Space Administration.

spacecraft mass constraint, mapping the required EIRP to a spacecraft mass (via the required power and transmitting antenna diameter). We do not map EIRP to a mass requirement, and instead focus on trade-offs for two spacecraft with fixed EIRP.

II. Link Equation

The received signal power over a free-space communications link may be factored as

$$P_r = P_t \left(\frac{\pi D_t D_r}{4R\lambda} \right)^2 \eta \tag{1}$$

$$= E \left(\frac{D_r}{4R} \right)^2 \eta \tag{2}$$

where

- P_t is the transmitted power,
- λ is the carrier wavelength,
- D_t is the transmit antenna diameter,
- D_r is the receive antenna diameter,
- η is the system efficiency $(0 \le \eta \le 1)$,
- R is the range, and
- E is the EIRP $(E = P_t (\pi D_t / \lambda)^2)$.

We assume the system efficiency η is not a function of the range, noise power, or antenna diameter. This is a simplification: for example, the pointing error may increase with range for a beacon-aided pointing system, losses due to blocking, or saturation; will depend on the noise power; and antenna efficiencies may depend on the antenna diameter. Nonetheless, it is sufficient for our purpose, which is to focus on the impact of space loss, the dominant loss term. We assume the noise power, P_n, is proportional to the receive aperture area,

$$P_n = \alpha_b \pi D_r^2 / 4 \tag{3}$$

where α_b is the noise power spatial density at the receiver in W/m^2. This is the case, for example, when the noise is dominated by spatially invariant sky radiance. In that case, the noise power density may be expanded as [3]

$$\alpha_b = B \Omega \Delta\lambda \eta_b$$

where B is the noise irradiance, Ω is the field of view, $\Delta\lambda$ is the receiver bandwidth, and η_b is the system efficiency with respect to the noise (the fraction of incident background photons that are detected). For example, a deep-space operating point may have $B = 5 \times 10^{-3}$ W/cm^2/sr/μm, $\Omega = 10^{-9}$ sr, $\Delta\lambda = 2 \times 10^{-4}$ μm, and $\eta_b = 0.1$, yielding $\alpha_b = 1$ pW/m^2.

We observe that the receiver bandwidth for the direct-detection optical system is generally invariant with data rate, in marked contrast to an RF system. The predetection optical bandpass filter sets the noise bandwidth. There are limitations (present technology and fundamental) to transmission efficiency versus bandwidth of this filter, especially when

receiving a signal spatially disturbed by atmospheric turbulence. Thus, lower data rate direct-detection links in low-SNR regimes are typically achieved by *increasing* modulation bandwidth by increasing the PPM order to match the optical noise bandwidth.

III. Capacity/Critical Range

In this section, we derive several approximations to the PPM capacity and show that at high SNR the capacity goes as $1/R^2$, while at low SNR it goes as $1/R^4$. Recall that we presume, throughout, that the optical link utilizes PPM (a form of intensity modulation) and a direct-detection photon-counting receiver. This is an efficient scheme to achieve the high photon efficiencies required by a deep-space link and represents the current state of the art.

In the infrared regime, the system bandwidth is limited by the bandwidths of the available electrical and optical components. This bandwidth is large (several GHz), and, over a broad range of interest, the capacity is limited primarily by the peak and average power constraints and not by the bandwidth. The capacity of the peak and average power-constrained optical channel (with no bandwidth limit) is [4]

$$C = \Big(\big(P_r + P_n/M\big) \log_2\big(1 + MP_r/P_n\big) - \big(P_r + P_n\big) \log_2\big(1 + P_r/P_n\big) \Big) / E_\lambda \quad \text{b/s} \tag{4}$$

where powers P_r, P_n are in watts, $E_\lambda = hc/\lambda$ is the energy per photon in joules, h is Planck's constant, c is the speed of light, and M is the peak-to-average power ratio. In order to further simplify analysis and to enable a clear view of the trade-offs between the signal and noise power, we derive an approximation to Equation (4). Let

$$C_1 = \big(M-1\big) P_r^2 / \big(2 \ln(2) P_n E_\lambda\big)$$
$$C_0 = \log_2(M) P_r / E_\lambda .$$

It is straightforward to show that

$$\lim_{P_r \to 0} \frac{C}{C_1} = 1 \quad \lim_{P_r \to \infty} \frac{C}{C_1} = 0$$
$$\lim_{P_r \to \infty} \frac{C}{C_0} = 1 \quad \lim_{P_r \to 0} \frac{C}{C_0} = 0.$$

This motivates defining a function C' as

$$\frac{1}{C'} = \frac{1}{C_0} + \frac{1}{C_1}.$$

Clearly, $\frac{C}{C'} \to 1$ as $P_r \to 0$ and as $P_r \to \infty$. We also have $C' \asymp C$ everywhere, or

$$C \asymp \frac{1}{E_\lambda \ln(2)} \left(\frac{P_r^2}{P_r \frac{1}{\ln(M)} + P_n \frac{2}{M-1}} \right) \quad \text{b/s}. \tag{5}$$

From Equation (1), $P_r \propto 1/R^2$, hence, from Equation (5), we see that the capacity may be divided into two regimes: for $P_r \gg 2P_n \ln M/M$, the capacity goes as $1/R^2$, for $P_r \ll 2P_n \ln M/M$, the capacity goes as $1/R^4$. Substituting Equations (1) and (3) into Equation (5), the crossover between the R^2 and R^4 regimes occurs at the *critical range*

$$R^* \approx \sqrt{\frac{\eta E(M-1)}{8\pi\alpha_b \ln M}}. \tag{6}$$

That is, we have

$$C \approx \begin{cases} \dfrac{1}{R^2}\dfrac{ED_r^2\eta\log_2(M)}{16E_\lambda} & ,R < R^* \\ \dfrac{1}{R^4}\dfrac{E^2D_r^2\eta^2(M-1)}{128\pi\alpha_b E_\lambda \ln(2)} & ,R > R^*. \end{cases} \tag{7}$$

Figure 1 illustrates Equation (4), its approximation Equation (5), the asymptotes Equation (7), and their intercept, R^*, for the parameters listed in Table 1 on page 8.

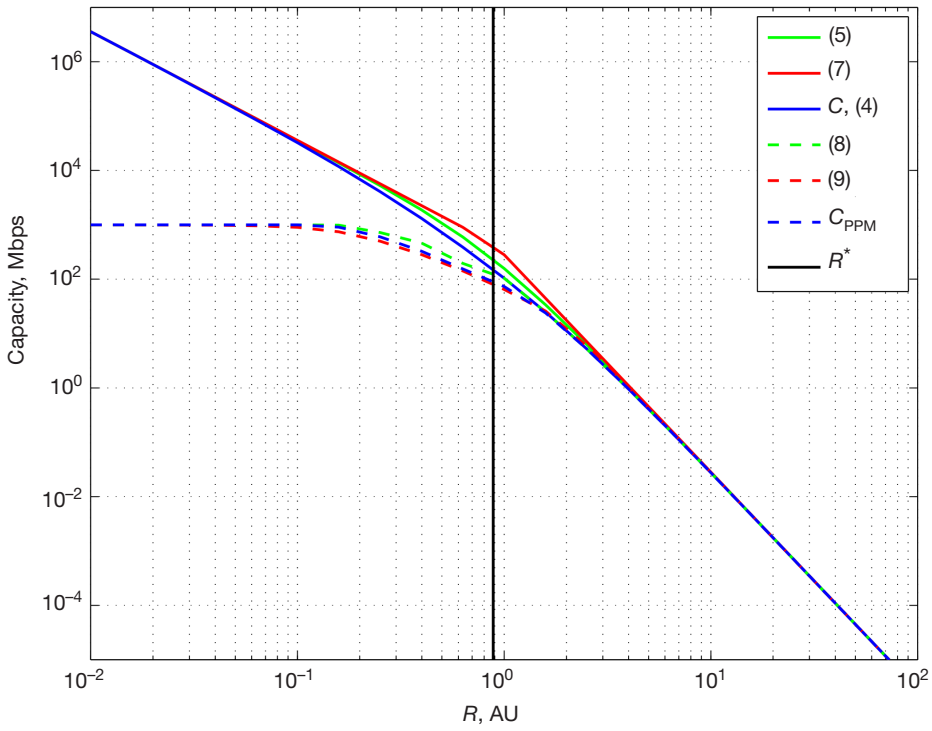

Figure 1. Capacity of the peak and average power-constrained photon-counting channel [Equation (4)], its approximation given by Equation (5), the asymptotes [Equation (7)], and the critical range R^*. Also illustrated are the Poisson PPM capacity, C_{PPM}, its bound [Equation (8)], and its approximation [Equation (9)]. Parameters are given in Table 1 on page 8.

Bandwidth Constraint

A deep-space optical link operates efficiently at large M. This may be implemented efficiently with PPM of order M. When implementing PPM, bandwidth constraints place a limit on the minimum supportable slot width T_s. This in turn bounds the maximum achievable data rate. Here, we extend approximation [Equation (5)] to the case of PPM with finite slot widths.

Let C_{PPM} denote the capacity of the PPM channel of order M with a finite slot width T_s. There is no closed-form expression for C_{PPM} in general [5]. However, we have the bound

$$C_{\mathrm{PPM}} \leq \min\left\{C, \frac{\log_2(M)}{MT_s}\left(1-\exp(-MP_rT_s/E_\lambda)\right)\right\} \quad \text{b/s.} \tag{8}$$

The first term is the unconstrained bandwidth bound; the second is the exact PPM capacity for the case $P_n = 0$, and captures the bandwidth constraint. Similar to the simplification in Section III, let $C_\infty = \frac{\log_2(M)}{MT_s}$, and define

$$\frac{1}{C''} = \frac{1}{C} + \frac{1}{C_\infty}.$$

Then $\frac{C_{\mathrm{PPM}}}{C''} \to 1$ as $P_r \to 0$ and as $P_r \to \infty$, and $C'' \approx C_{\mathrm{PPM}}$, or

$$C_{\mathrm{PPM}} \approx \frac{1}{\ln(2)E_\lambda}\left(\frac{P_r^2}{P_r\frac{1}{\ln(M)} + P_n\frac{2}{M-1} + P_r^2\frac{MT_s}{\ln(M)E_\lambda}}\right) \quad \text{b/s}. \tag{9}$$

This provides a simple approximation to the PPM capacity, capturing the bandwidth constraint (finite T_s). Figure 1 illustrates C_{PPM}, computed numerically, the bound [Equation (8)], and approximation [Equation (9)], for the parameters listed in Table 1 (page 8). In this article, our focus is on transitions that typically occur in the region where the bandwidth constraint is inactive; hence, in the remainder we assume the bandwidth constraint is inactive and use Equation (4), or its approximations.

IV. Critical Receive Diameter

Suppose we have a target capacity C, and a system design that achieves this capacity with a specified (E, D_r, η), as given by Equation (7). From Equation (7), we see that we can achieve the same capacity while decreasing the spacecraft burden (the EIRP E), by increasing the system efficiency η, the PPM order M, or the receive aperture D_r. Here, we focus on changing the receive aperture (typically, increasing the PPM order is limited by achievable peak power and the system efficiency is maximized up to limits of complexity). A systems engineer would like to know: With other system parameters fixed (η, M, α_b), *by how much can we decrease the EIRP for a given increase in D_r, while keeping the capacity constant?*

From Equation (7), we see that if $R > R^*$, then an X-dB increase in D_r allows an X-dB decrease in E, whereas, if $R < R^*$, an X-dB increase in D_r allows a $2X$-dB decrease in E. We may alternately frame this in terms of a critical receive diameter for a target capacity as follows. Put

$$P_r = \alpha_r \frac{\pi D_r^2}{4} \tag{10}$$

where $\alpha_r = E\eta/(4\pi R^2)$ is the average received signal spatial power density in W/m^2 [analogous to α_b in Equation (3)]. Suppose the signal and noise power densities (α_r, α_b) are fixed. Solving for D_r in Equation (5), we have

$$D_r = \sqrt{\frac{4\ln(2)CE_\lambda}{\pi\alpha_r}\left(\frac{1}{\ln(M)} + \frac{2}{(M-1)}\frac{\alpha_b}{\alpha_r}\right)}. \tag{11}$$

Hence, for

$$\frac{\alpha_b}{\alpha_r} = \frac{P_n}{P_r} \gg \frac{M-1}{2\ln M},$$

we have $D_r \propto 1/E$, and for

$$\frac{\alpha_b}{\alpha_r} \ll \frac{M-1}{2\ln M},$$

we have $D_r \propto 1/\sqrt{E}$. The intersection of these regions — where $\alpha_b/\alpha_r = (M-1)/(2\ln M)$ — occurs at

$$D_r^* = \frac{2}{\ln M}\sqrt{\frac{CE_\lambda \ln(2)(M-1)}{\pi\alpha_b}}. \tag{12}$$

We refer to this as the *critical receive diameter*. For a target C in noise α_b, if $D_r < D_r^*$, increasing the receive aperture allows a corresponding scaling of the EIRP. If $D_r > D_r^*$, then increasing the receive aperture allows only a square-root scaling of the EIRP. For example, Figure 2 illustrates the required D_r given by Equation (11) to support $C = 10$ Mbps as a function of α_r (a scaled measure of EIRP), for the case $M = 128$, $\alpha_b = 1\text{pW/m}^2$, and $\lambda = 1.55$ μm. In this case, the critical diameter is $D_r^* = 6.3$ m.

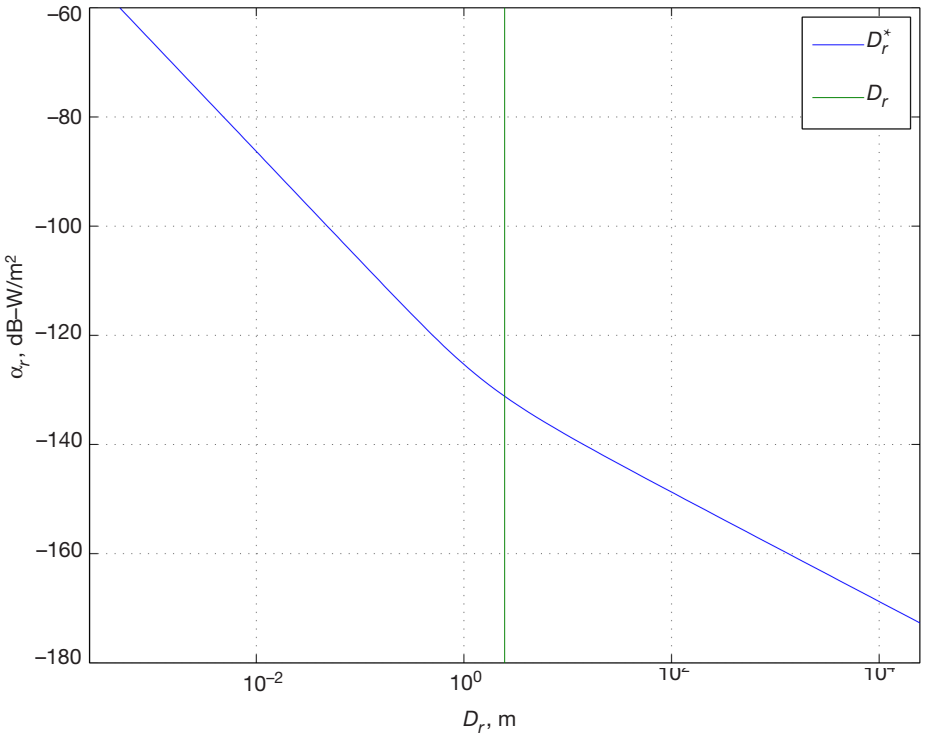

Figure 2. Required signal spatial power density α_r as a function of the receive diameter D_r, for an optical system with $M = 128$, $\alpha_b = 1$ pW/m^2, $\lambda = 1.55$ μm, $C = 10$ Mbps. The maximum efficient receive diameter, $D_r^* = 6.3$ m, illustrates a break-point in the log-domain slope.

V. RF and Optical Capacity Crossover

In this section, we draw comparisons between the capacity of coherent microwave (RF) and direct-detected infrared (optical) systems. We first review the capacity of an RF system. On the RF channel, we presume the noise power is dominated by the thermal noise of the receiver amplifier, as is the case for the Deep Space Network, and approximate it as

$$N_0 W = kTW$$

where k is Boltzmann's constant, T is the system noise temperature, and W is the system bandwidth. Under this assumption, the noise power does not scale with the aperture diameter.

The capacity of the RF link with no bandwidth constraint, or an inactive bandwidth constraint, is [7]

$$C^{(r)} = \frac{P_r}{\ln(2) N_0} \quad \text{b/s} \tag{13}$$

(we continue to use C, C_{PPM} to denote optical capacities and will use $C^{(r)}$ to denote the RF capacity). As is well known, we see from Equation (1) that for a fixed system (transmitted power, apertures, and efficiencies), the capacity goes as $1/R^2$. With a bandwidth of W Hz, the capacity goes as

$$C^{(r)}(W) = W \log_2\left(1 + \frac{P_r}{N_0 W}\right) \quad \text{b/s},$$

which, in the power-constrained region (small $P_r/N_0 W$) also goes as $1/R^2$.

We are now in a position to compare RF and optical communication systems. When making system comparisons, we will differentiate the optical parameters with a superscript as $E^{(o)}, D_r^{(o)}, \ldots$ and the RF parameters as $E^{(r)}, D_r^{(r)}, \ldots$ (no superscripts will be used when the parameters are nonspecific or clear from context). Suppose we have two fixed systems, and consider their performance as a function of the range. We assume that, due to the EIRP gain of infrared over microwave, $C > C^{(r)}$ at short ranges, and, since C goes as $1/R^4$ at sufficiently large R, a crossover to a region with $C^{(r)} > C$ at large range. Hence, there is some critical range R' where $C = C^{(r)}$. This crossover must occur in the $R > R^*$ region for the optical system, and typically in the average power-constrained region of the RF system. Hence, setting the $R > R^*$ equation of Equation (7) equal to Equation (13) and solving yields an approximation to R':

$$R' \approx \sqrt{\frac{N_0(M-1)}{8\pi E_\lambda \alpha_b}} \frac{E^{(o)}}{\sqrt{E^{(r)}}} \frac{D_r^{(o)}}{D_r^{(r)}} \frac{\eta^{(o)}}{\sqrt{\eta^{(r)}}}. \tag{14}$$

In the following section, we provide an example of the crossover for representative state-of-the-art systems.

Example: State-of-the-Art RF and Optical Links

In this section, we compare two specific candidate links: a Ka-band RF link at 32 GHz and an optical link in the near-infrared at 193.5 THz (1.55 μm). These represent current state-of-the-art candidates for a deep-space telecommunications link. Table 1 summarizes the system parameters. We select the RF transmit diameter to be $D_t^{(r)} = 3.0$ m, and RF transmit power to be $P_t^{(r)} = 35$ W, corresponding to a Ka-band Mars Reconnaissance Orbiter link. For the optical system, we choose a transmit diameter and power of $D_t^{(o)} = 22$ cm, and $P_t^{(o)} = 4$ W, corresponding to the Deep-Space Optical Transceiver concept. We select $D_r^{(r)} = 34$ m, corresponding to a Deep Space Network antenna, and $D_r^{(o)} = 11.8$ m, corresponding to the Large Binocular Telescope.

Table 1. Sample Ka-band and infrared link parameters.

Ka-band Link		
f	Carrier frequency	32.0 GHz
D_t	Transmit diameter	3.0 m
D_r	Receiver diameter	34.0 m
η	System efficiency	–10.88 dB
N_0	Noise spectral density	–178.45 dB-mW/Hz
W	Bandwidth	500 MHz
P_t	Transmit power	35 W
Near-Infrared Link		
λ	Wavelength	1.55 μm
D_t	Transmit diameter	22.0 cm
D_r	Receiver diameter	11.8 m
η	System efficiency	–16.74 dB
α_b	Noise spatial density	1.0 pW/m^2
T_s	Slot width	0.5 ns
P_t	Transmit power	4 W

For the Ka-band link, we assume a system efficiency of –10.88 dB[1], and take the noise spectral density to be $N_0 = -178.45$ dB-mW/Hz, corresponding to a noise temperature of 103.58 K [6, Appendix 4A]. For the infrared link, we assume a system efficiency of –16.74 dB.[2] The noise power spatial density is taken to be $\alpha_b = 1$ pW/m^2.

Figure 3 illustrates $C^{(r)}$, $C^{(r)}(W)$, C, and C_{PPM} as a function of the range (in AU) for the parameters described above. For the C_{PPM} curve, we set $T_s = 0.5$ ns, near the limit of current technology, and we optimize over $4 \leq M \leq 128$. For the C curve, we set $M = 128$. For the $C^{(r)}(W)$ curve, we assume $W = 500$ MHz, occupying the entire allocated Ka-band. We see the knee between the two regions of the optical capacity at $R^* = 0.89$ AU. The bandwidth limits constrain the maximum achievable rates, but are inactive for data rates less than $\approx$100 Mbps.

[1] We add a 1.0 dB code imperfectness to the loss in [6, Appendix 4A] to be consistent with the loss treatment for optical.

[2] Losses are drawn from "Deep-Space Optical Transceiver Concept Review," Jet Propulsion Laboratory, Pasadena, California, August 8, 2010.

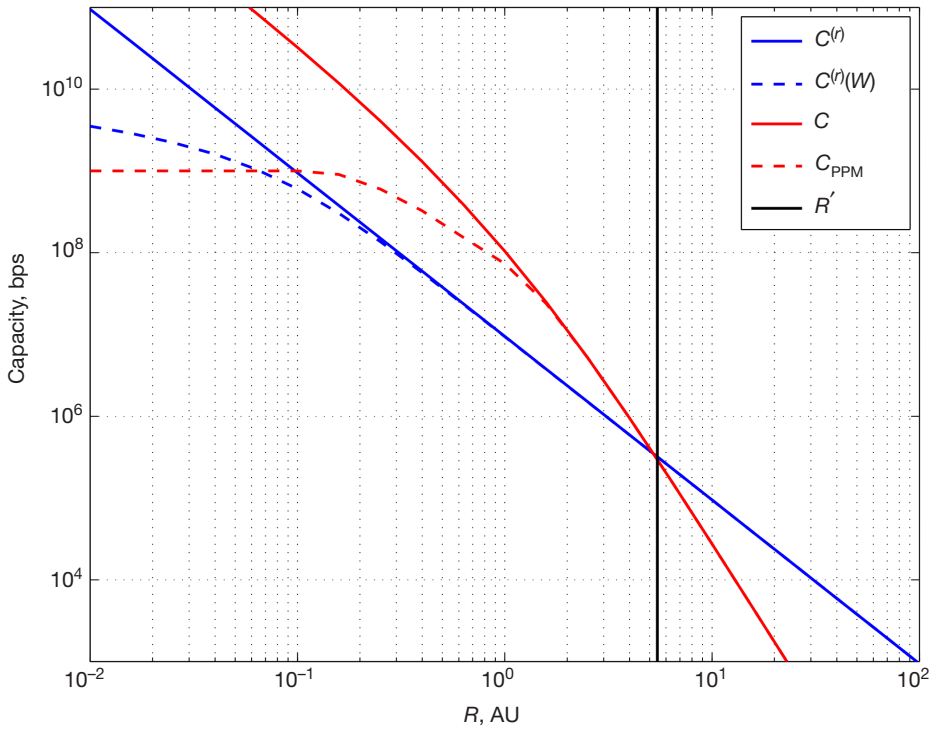

Figure 3. RF and optical capacities $C^{(r)}$, $C^{(r)}(W)$, C, $C(T_s)$, as a function of range R. Crossover at R'.

Changing assumptions about noise powers (e.g., day or night operations at a ground station) or system efficiencies will shift the curves up or down, but the relative shapes will persist. Beyond a certain range, the optical signal power will fall below the noise floor introduced by background radiance. Narrowing the optical bandwidth would reduce the background radiance, but this goes against increasing the modulation bandwidth for high photon efficiency by increasing the PPM order for lower data rates. In the region where $P_r \ll 2P_n \ln M/M$, the capacity goes as $1/R^4$, and the optical system will, for sufficiently large R, no longer outperform the RF system. Using the approximation of Equation (14), we obtain $R' \approx 5.45$ AU, in agreement with Figure 3.

VI. Conclusions

We derived a useful approximation to the Poisson PPM capacity, Equation (9), which reduces to Equation (5) when the bandwidth constraint is inactive. Using this, we show the capacity of a PPM direct-detected optical link goes as $1/R^2$ at high SNR and $1/R^4$ at low SNR. This implies that at sufficiently large range, a fixed optical system (transmit and receive terminals) will have a lower capacity than a fixed RF system. This is primarily due to the fact that the noise bandwidth is set by an optical filter bandwidth that is not reduced with decreasing data rate. The larger question we're after is this: If one wants to establish a link at a given data rate and range, which communication system imposes less of a burden on the spacecraft, optical or RF? To determine this requires a mapping of EIRP to a measure of the burden, which we may take to be the mass. These results may aid that study by establishing straightforward relationships between EIRP, noise power, range, and capacity.

References

[1] M. Toyoshima, W. R. Leeb, H. Kunimori, and T. Takano, "Comparison of Microwave and Light Wave Communication Systems in Space Applications," *Optical Engineering*, vol. 46, no. 1, p. 015003, January 30, 2007.

[2] W. D. Williams, M. Collins, D. M. Boroson, J. Lesh, A. Biswas, et al., "RF and Optical Communications: A Comparison of High Data Rate Returns from Deep Space in the 2020 Timeframe," NASA/TM–2007-214459, NASA Glenn Research Center, Cleveland, Ohio, pp. 1–16, March 2007.
http://ntrs.nasa.gov/archive/nasa/casi.ntrs.nasa.gov/20070017310.pdf

[3] A. Biswas and S. Piazzolla, "Deep Space Optical Communications Downlink Budget from Mars: System Parameters," *The Interplanetary Network Progress Report*, vol. 42-154, Jet Propulsion Laboratory, Pasadena, California, pp. 1–38, August 15, 2003.
http://ipnpr.jpl.nasa.gov/progress_report/42-154/154L.pdf

[4] A. D. Wyner, "Capacity and Error Exponent for the Direct Detection Photon Channel, Part I," *IEEE Transactions on Information Theory*, vol. 34, no. 6, pp. 1449–1461, November 1988.

[5] B. Moision and J. Hamkins, "Deep-Space Optical Communications Downlink Budget: Modulation and Coding," *The Interplanetary Network Progress Report*, vol. 42-154, Jet Propulsion Laboratory, Pasadena, California, pp. 1–28, August 15, 2003.
http://ipnpr.jpl.nasa.gov/progress_report/42-154/154K.pdf

[6] W. D. Williams, M. Collins, R. Hodges, R. S. Orr, O. S. Sands, L. Schuchman, and H. Vyas, "High-Capacity Communications from Martian Distances," NASA/TM–2007-214415, NASA Glenn Research Center, Cleveland, Ohio, pp. 1–162, December 2007.
http://ntrs.nasa.gov/search.jsp?R=20080012561

[7] T. M. Cover and J. A. Thomas, *Elements of Information Theory*, New York: John Wiley and Sons, 1991.